IVYSPRING INTERNATIONAL PUBLISHER

Theranostics

2012; 2(10):999-1009. doi: 10.7150/thno.5276

Research Paper

Evaluation of an [^{18}F]AlF-NOTA Analog of Exendin-4 for Imaging of GLP-1 Receptor in Insulinoma

Dale O. Kiesewetter[1*], Ning Guo[1, 2*], Jinxia Guo[1, 2], Haokao Gao[1,3], Lei Zhu[1,4], Ying Ma[1], Gang Niu[1]✉, Xiaoyuan Chen[1]✉

1. Laboratory of Molecular Imaging, National Institute of Biomedical Imaging and Bioengineering, NIH, Bethesda, MD 20892, USA
2. Department of Biomedical Engineering, Huazhong University of Science and Technology, Wuhan, Hubei, China 430074
3. Department of Cardiology, Xijing Hospital, the Fourth Military Medical University, Xi'an, China 710032
4. Center for Molecular Imaging and Translational Medicine, School of Public Health, Xiamen University, Xiamen, China 361005

* co-first authors

✉ Corresponding author: Dr. Xiaoyuan Chen, shawn.chen@nih.gov; or Dr. Gang Niu, niug@mail.nih.gov

© Ivyspring International Publisher. This is an open-access article distributed under the terms of the Creative Commons License (http://creativecommons.org/licenses/by-nc-nd/3.0/). Reproduction is permitted for personal, noncommercial use, provided that the article is in whole, unmodified, and properly cited.

Received: 2012.09.22; Accepted: 2012.10.16; Published: 2012.10.17

Abstract

Introduction: The GLP-1 receptor plays an important role in glucose homeostasis and thus is a very important target for diabetes therapy. The receptor is also overexpressed in insulinoma, a tumor of pancreatic beta-cells. We previously evaluated two fluorine-18-labeled analogs of exendin-4 prepared by conjugation with [^{18}F]FBEM (N-[2-(4-[^{18}F]fluorobenzamide) ethyl]maleimide). Both compounds demonstrated good tumor uptake, but the synthesis of the radiotracers was time consuming. To overcome this challenge, we developed a NOTA analog and performed radiolabeling using aluminum [^{18}F]fluoride complexation.

Methods: Cys^{40}-exendin-4 was conjugated with NOTA mono N-ethylmaleimide. [^{18}F]AlF conjugation was conducted and the radiolabeled product purified by preparative HPLC. Dynamic and static PET imaging scans were conducted on nude mice with established INS-1 xenografts. Uptake of tumor and other major organs in static images was quantitated (%ID/g) and comparison with blocking studies was made. PET quantification was also compared with ex vivo biodistribution results.

Results: The radiosynthesis provided [^{18}F]AlF-NOTA-MAL-cys^{40}-exendin-4 in 23.6 ± 2.4 % radiochemical yield (uncorrected, n = 3) after HPLC; the process required about 55 min. The specific activity at time of injection ranged from 19.6 to 31.4 GBq (0.53-0.85 Ci)/μmol. Tumor uptake had reached its maximum (16.09 ± 1.18% ID/g, n = 4) by 5 min and remained nearly constant for the duration of the study. Kidney uptake continued to increase throughout the entire one hour time course. Pre-injection of exendin-4 caused a marked reduction in tissue uptake with the major exception of liver and kidneys, in which uptake was not affected. HPLC analysis of the radioactive components in extracts of the tumor and plasma showed primarily parent compound at 60 min post-injection, whereas extracts of kidney and urine contained exclusively one polar radioactive component.

Conclusion: The radiotracer is prepared in a simple one-step procedure and obtained in high specific activity after HPLC purification. [^{18}F]AlF-NOTA-MAL-exendin-4 shows high tumor uptake and highly selective GLP-1 tissue uptake (INS-1 tumor, lung, pancreas), but still suffers from high kidney uptake.

Key words: [^{18}F]fluoride, insulinoma, exendin-4, PET

Introduction

The development of radiotracers for use in positron emission tomography (PET) requires consideration of biological and chemical issues [1]. In the first place, the tracer must image a target of relevance to human disease either as a research tool to better understand the disease or as a clinical tool to benefit individual patients. The radiotracer must exhibit specific binding to the desired target, an appropriate signal to noise ratio to allow visualization of desired target over background, pharmacokinetics appropriate for the biological system and the incorporated radionuclide, and metabolic kinetics and clearance that do not interfere with image interpretation. In addition, the radiotracer must be synthesized using a chemical procedure that is robust and easily transferable to other facilities.

We have been interested in the development of a peptide based imaging agent for GLP-1R (glucagon-like peptide type 1 receptor). Endogenously produced GLP-1 interacts with GLP-1R to cause the production of insulin in response to ingestion of food [2]. GLP-1R is present in the beta-cells of the pancreas [3] and in insulinoma (a neuroendocrine tumor of the pancreas) [4]. GLP-1R is also expressed in injured myocardium and has become a therapy target in cardiovascular disease [5]. Insulinoma is relatively rare and the tumor is generally quite small when the symptoms appear. Typical clinical imaging scans using CT, echography, or MRI are usually unable to detect the tumors [6]. An imaging agent appropriate for the GLP-1R system would be useful in assisting with diagnosis of insulinoma and potentially in the study of diabetes.

GLP-1 is a very unstable peptide, presumably by evolutionary design, such that the signal from binding of a radioligand to GLP-1 could be rapidly turned off by enzymatic degradation of the peptide [7]. We began our studies using a synthetic peptide (EM3106B) that contains two internal lactams designed to increase the stability of the peptide [8]. EM3106B contains a single terminal cysteine residue to allow radiolabeling with the prosthetic reagent [^{18}F]FBEM (N-[2-(4-[^{18}F]fluorobenzamido)ethyl] maleimide) [9]. This radiolabeled peptide showed excellent tumor uptake in an insulinoma xenograft model [10].

We next investigated exendin-4, a 39 amino acid residue linear peptide discovered in the saliva of a lizard, as the backbone for a GLP-1 tracer [11] because we considered the synthesis of derivatives of EM3106B as more challenging. Exendin-4 has been utilized by others as a scaffold for imaging insulinoma and for tumor therapy with radiometals [12-14]. Exendin-4 is used therapeutically in diabetes because of its reasonable biological half-life and high efficacy after subcutaneous injection. We synthesized analogs containing cysteine at either the C-terminus or N-terminus. The C-terminal analog, [^{18}F]FBEM-cys^{40}-exendin-4 showed high tumor uptake and high tumor to background radioactivity ratio for all tissues except kidneys [15]. Kidney uptake did diminish over the course of two hours in the mouse xenograft model, however some abdominal uptake was observed. This abdominal uptake could limit the ability to visualize insulinoma in the area of the pancreas. [^{18}F]FBEM-cys^{40}-exendin-4 also showed specific binding to GLP-1R in a cardiac model of ischemia/reperfusion injury [16].

Despite the encouraging results for [^{18}F]FBEM-cys^{40}-exendin-4, we believe that further improvements can still be achieved. Our inability to define the abdominal structures with low uptake may compromise the usefulness for pancreatic imaging. However, the tedious radiosynthesis of the [^{18}F]FBEM prosthetic group was perceived as the bigger impediment to more widespread use of the tracer. In this study, we developed an exendin-4 analog, which can be radiolabeled using complexation with aluminum [^{18}F]fluoride [17], and evaluated its properties in a mouse xenograft model of insulinoma.

Methods

General: High performance liquid chromatography (HPLC,) semi-preparative and analytical, was performed on Vydac C-18 columns (Grace Davison Discovery Sciences, Deerfield, IL, USA) with gradient elution of mixtures of solvent A (0.1% TFA in water) and solvent B (0.1% TFA in CH_3CN). HPLC-MS was performed on a Waters Qtof time-of-flight mass spectrometer coupled with a Waters Acquity UPLC system (Waters, Inc, Milford, MA). UPLC separation utilized a Acquity BEH Shield RP18 column (150 mm x 2.1 mm, Waters, Milford, MA, USA) with eluent A (5% CH3CN, 0.1% formic acid, and 2 mM ammonium formate in water) and eluent B (5% water, 0.1% formic acid, and 2 mM ammounium formate in CH_3CN. The flow was 0.35 mL/min and a linear gradient began at 100% A to 60 % A at 5 min and then held at 60% A for 5 min.

Synthesis of NOTA-MAL-exendin-4 analogs.

Cys^{40}–exendin-4 and cys^{0}-exendin-4 were synthesized by C.S. Bio (Menlo Park, CA). The exendin-4 sequence for the cys^{40} analog is His-Gly-Glu-Gly-Thr-Phe-Thr-Ser-Asp-Leu-Ser-Lys-Gly-Met-Glu-Glu-Glu-Ala-Val-Arg-Leu-Phe-Ile-Glu-

Trp-Leu-Lys-Asn-Gly-Gly-Pro-Ser-Ser-Gly-Ala-Pro-Pro-Pro-Ser-Cys-NH_2. Reactions to add the NOTA group to either isomer were conducted on a few milligram scale using the same procedure. To a vial charged with cys^{40}-exendin-4 (6.77 mg, 1.57 µmol) was added a solution of (2.16 mg, 3.2 µmol) NOTA-maleimide mono TFA, mono hexafluorophosphate salt (Chematech, Dijon, France) in 200 µL CH_3CN. Then, 1.3 mL of degassed 0.1% sodium ascorbate in phosphate buffered saline (PBS) was added and the mixture allowed to stand at room temperature for 2 – 3 h. The mixture was treated with 0.1% TFA (200 µL) and subjected to semi-preparative HPLC in two portions. The conditions were: column Vydac C-18 (#218TP510, 10 mm x 250 mm), flow rate 5 mL/min; elution was 5 min isocratic at 25% B, then a gradient from 25% B to 55% B at 30 min, to 65% at 35 min. The product eluting at about 17 min was collected, combined with subsequent purification runs and lyophilized. Yield of recovered of NOTA-MAL-cys^{40}-exendin-4 was 6.56 mg (1.39 µmol, 88.6%). For the cys^0-isomer, from 3.44 mg precursor was obtained 3.4 mg NOTA-MAL-cys^0-exendin-4 (92%). Yields are based on the mass spectral determined molecular weight and assume no counter ions are present. HPLC-MS (described above) calculated $C_{205}H_{314}N_{56}O_{68}S_2$: 4712.2. Found (cys^0-isomer); deconvolution 4714, MS/MS fragments 396, 299, 202 consistent with C-terminal fragmentations. Found (cys^{40} isomer); deconvolution 4714, MS/MS 924, 730 consistent with C-terminal fragments containing the NOTA substructure.

Radiochemical synthesis of [^{18}F]AlF-NOTA-MAL-cys^x-exendin-4.

A 2 mL centrifuge tube was charged with 3 µL of a solution of aluminum chloride (2 mM) in 0.5 M NaOAc (pH = 4). Cyclotron target water containing [^{18}F]fluoride (up to 40 µL containing up to 1110 MBq) was added, followed by the substrate (70 µg) in 40 µL of 0.5 M sodium acetate buffer (pH = 4), and 200 µL CH_3CN. The resulting solution was heated at ~ 90 °C for 10 min. The reaction mixture was then cooled, diluted with 200 µL 0.1% TFA and injected onto a semi-preparative Vydac HPLC column (as described above). The elution conditions began with a 5 min isocratic period at 25 % A followed by a linear gradient over 30 min to 55% A at a flow rate of 5 mL/min. The radioactivity peak eluting at ~17 min was collected. The radiochemical yield was calculated at this point, 35 min from start of the reaction. The product was isolated from the eluate using C-18 solid phase extraction (SPE) and the product subsequently re-eluted with 20% aqueous ethanol containing 10 mM HCl. This eluate was treated with 100 µL of 0.1 M NaOAc (pH = 4) and concentrated to about 200 µL total volume under a stream of argon. This sample was diluted with PBS for animal injections. The product isolation and formulation required about 20 min.

Quality control of [^{18}F]AlF-NOTA-MAL-cys^x-exendin-4.

A sample of the eluate from SPE was analyzed by analytical HPLC (Vydac C-18 (#218TP54), 4.6 mm x 250 mm, 1 mL/min). The eluent employed three components: A) water; B) CH_3CN; C) 1% TFA (129 mM) and 1 mM tetrasodium EDTA in water (unadjusted pH measured 0.9). Initial conditions-- A-65%, B-25%, C-10% -- were maintained for 5 min. Subsequently a linear gradient from 25% B to 55% B, while maintaining C at 10%, was run over 20 min. UV absorbance (210, 230, 250, 280 nm) and radioactivity (Flow-count detector, Bioscan, Washington, DC) were monitored. Specific activity was estimated at each of the wavelengths by comparison with a standard curve based on FBEM-cys^{40}-exendin-4.

Mass spectral analysis of [^{18}F]AlF-NOTA-MAL-cys^{40}-exendin-4.

UPLC-MS analysis of the collected radioactive product revealed two major mass components. Deconvolution of the peptide spectra suggested the aluminum complex and aluminum fluoride complex of NOTA-MAL-cys^{40}-exendin-4 were these major components. Aluminum complex calculated $C_{205}H_{311}AlN_{56}O_{68}S_2$: 4736.1856; deconvolution 4739. Aluminum fluoride complex calculated: $C_{205}H_{312}AlFN_{56}O_{68}S_2$: 4756.1918; deconvolution: 4758.

Affinity determination in cell binding assays.

The binding affinities of NOTA-MAL-cys^{40}-exendin-4, FBEM-cys^{40}-exendin-4, and exendin-4 were assessed via a competitive cell binding assay using ^{125}I-GLP-1(7–36) (PerkinElmer, Waltham, MA, USA) as the GLP-1R specific radioligand. Experiments were performed on duplicate samples of rat INS-1 cells. The best-fit 50% inhibitory concentrations (IC_{50}) for the INS-1 cells were calculated by fitting the data with nonlinear regression using GraphPad Prism (GraphPad, La Jolla, CA, USA).

Stability in plasma.

[^{18}F]AlF-NOTA-MAL-cys^{40}-exendin-4 was mixed with human plasma (200 µL). A 50 µL aliquot was removed at 0 min. The remainder was incubated at 37°C and additional aliquots of 50 µL were removed

at 30 and 60 min. The aliquots were mixed with an equal volume of CH_3CN, the layers were assayed to determine extraction efficiency, and a portion of the supernatant was subjected to radio-HPLC analysis, using same method as described for quality control. Radioactivity was determined using an on-line radioactivity detector or collection of 1-min fractions followed by gamma-counting (Wallach Wizard, Perkin-Elmer, Waltham, MA).

Cell culture and animal model.

Studies with live animals were conducted in compliance with the principles and procedures outlined in the Guide for the Care and Use of Laboratory Animals and were approved by the Institutional Animal Care and Use of the Clinical Center, NIH. Rat insulinoma INS-1-derived 832/13 cells were grown in RPMI-1640 medium supplemented with 10% fetal bovine serum, 100 IU/mL penicillin, and 100 µg/mL streptomycin (Invitrogen, Grand Island, NY, USA), and in a humidified atmosphere containing 5% CO_2 at 37°C. The INS-1 xenograft tumor models were developed in 5- to 6-week old female athymic nude mice (Harlan Laboratories, Frederick, MD, USA) by injection of 5×10^6 cells into the right shoulder. Tumor growth was quantitated by measuring perpendicular axes of the tumor using a caliper. The tumor volume was estimated from the formula: tumor volume=$a\times(b^2)/2$, where a and b are the tumor length and width, respectively, in millimeters. The mice underwent a small-animal PET scan when the tumor volume reached about 200 mm^3 (3–4 weeks after inoculation).

Static PET/CT Scans and Image Analysis.

Scans were conducted on an Inveon micro-PET/CT scanner (Siemens Medical Solutions, Malvern, PA, USA). [^{18}F]AlF-NOTA-MAL-cys^x-exendin-4 (3.44 ± 0.26 MBq, containing ~300 pmol peptide, estimated from average specific activity) was injected, via a tail vein under isoflurane anesthesia, into INS-1 tumor bearing mice. The animals underwent a 15-min CT scan followed by the PET scan using the same animal bed for image co-registration and ROI quantification. Each INS-1 tumor-bearing mouse was placed at the center of the field of view (FOV) focusing on the tumor location, where the highest detection sensitivity can be achieved. Static PET images were acquired at 0.5 h (5 min scan time) and 1 h (10 min scan time) after injection (p.i.) (n = 6/group). For the GLP-1R blocking experiment, exendin-4 (100 µg) was injected 10 min prior to injection of [^{18}F]AlF-NOTA-MAL-cys^{40}-exendin-4 (3.7 MBq) into INS-1 tumor-bearing mice and 10-min static PET images were acquired at the 1-h time point (n = 4/group). PET images were reconstructed with 2 iterations of 3-dimensional ordered-subsets expectation maximum (3D OSEM) with 14 subsets, followed by 18 iterations maximum a posteriori (MAP) algorithm with a smoothing parameter of 0.1.

Dynamic PET data acquisition and time activity curves.

Sixty-min dynamic PET data acquisitions were performed following tail-vein injection of ~3.7 MBq of [^{18}F]AlF-NOTA-MAL-Cys^{40}-exendin-4 under isoflurane anesthesia in INS-1 tumor-bearing mice. During the scanning, the body temperature of mice was maintained by a thermostat-controlled thermal heater. PET images were reconstructed with 3D OSEM as described above. Frame rates of dynamic image series were 10×30 s, 5×60 s, 5×120 s and 10×240 s. In PET image analysis, ROIs were drawn manually on individual tumor and correlative organs with Inveon Research Workplace (IRW) 3.0. The time–activity curves were derived by superimposing the ellipsoid volume of interest (VOI) to the target organs of each time frame of the entire 60-min dynamic image sequence. PET/CT fused images were acquired for accurate VOI quantification. The value of each time point represents the overall concentration of radioactivity in the tissue. The radioactivity concentrations (accumulation) within the tumor, muscle, liver, and kidneys were obtained from mean pixel values within the multiple ROI volume and then converted to MBq/mL/min using the calibration factor determined for the Inveon PET system. These values were then divided by the administered activity to obtain (assuming a tissue density of 1 g/mL) an image ROI-derived percentage injected dose per gram (%ID/g).

Kidney uptake blocking studies.

Immediately before injection of radiolabeled tracer, a separate group (n = 4) of anesthetized mice was injected with 0.1 mL L-polyglutamic acid solution (Sigma-Aldrich, St. Louis, MO, 3-18 kDa, 80 mg/mL in saline). Kidney uptake was quantified based on PET images. This study was conducted with non-tumor bearing mice.

Biodistribution studies and metabolite analyses.

Immediately after the 1 h static PET imaging for control and blocking studies, the tumor-bearing mice were euthanized and dissected. Blood, tumor, major organs, and tissues were harvested and wet-weighed. The radioactivity in the tissue was measured with a

γ-counter (Wallach Wizard, PerkinElmer, Waltham, MA, USA). The results were expressed as percentages of the injected dose per gram of tissue (%ID/g) for a group of four animals. For each mouse, the radioactivity of the tissue samples was calibrated against a known aliquot of the injected radiotracer. Values are expressed as mean ± SD. A subset of the collected tissues (tumor, plasma, kidneys, urine) was homogenized and extracted with a volume of CH_3CN equal to the weight of the sample. The mixtures were centrifuged and the supernatant separated from the pellet. Supernatants were analyzed by HPLC using on-line radioactivity detection or via collection of 1 min fractions and subsequent γ-counting.

Statistical analysis.

Quantitative data were expressed as mean ± SD. Means were compared using one-way analysis of variance and Student's t test. A p value < 0.05 was considered statistically significant.

Results

Chemistry and radiochemistry.

The NOTA-derivatized precursors were synthesized by reaction with the commercially available mono ethylmaleimide amide of NOTA (figure 1). Because our previous work showed that the cys^{40} isomer had higher tumor uptake than the cys^{0} analog [15], we focused on this cys^{40} isomer. The product was purified by preparative HPLC and characterized by HPLC-MS. Although the product appeared as a single peak by HPLC, the mass spectrum suggested some minor impurities that were neither separated nor identified.

The radiochemical synthesis was conducted using aqueous [^{18}F]fluoride directly from the cyclotron target and a NaOAc buffer at pH 4 containing $AlCl_3$ and NOTA-derivatized peptide. The radiochemical yield after HPLC purification was 23.6 ± 2.4 % (n = 3, uncorrected). The specific activity ranged from 15.9 to 31.4 GBq/μmol at time of measurement (prior to animal studies). The HPLC purification did not separate the radiochemical product from non-fluorinated complex or from non-complexed NOTA-MAL-cys^{40}-exendin-4. The only identifiable components by LC-MS were the Al-NOTA-MAL-cys^{40}-exendin-4 complex (FW 4739) and the AlF-NOTA-MAL-cys^{40}-exendin-4 complex (FW 4758).

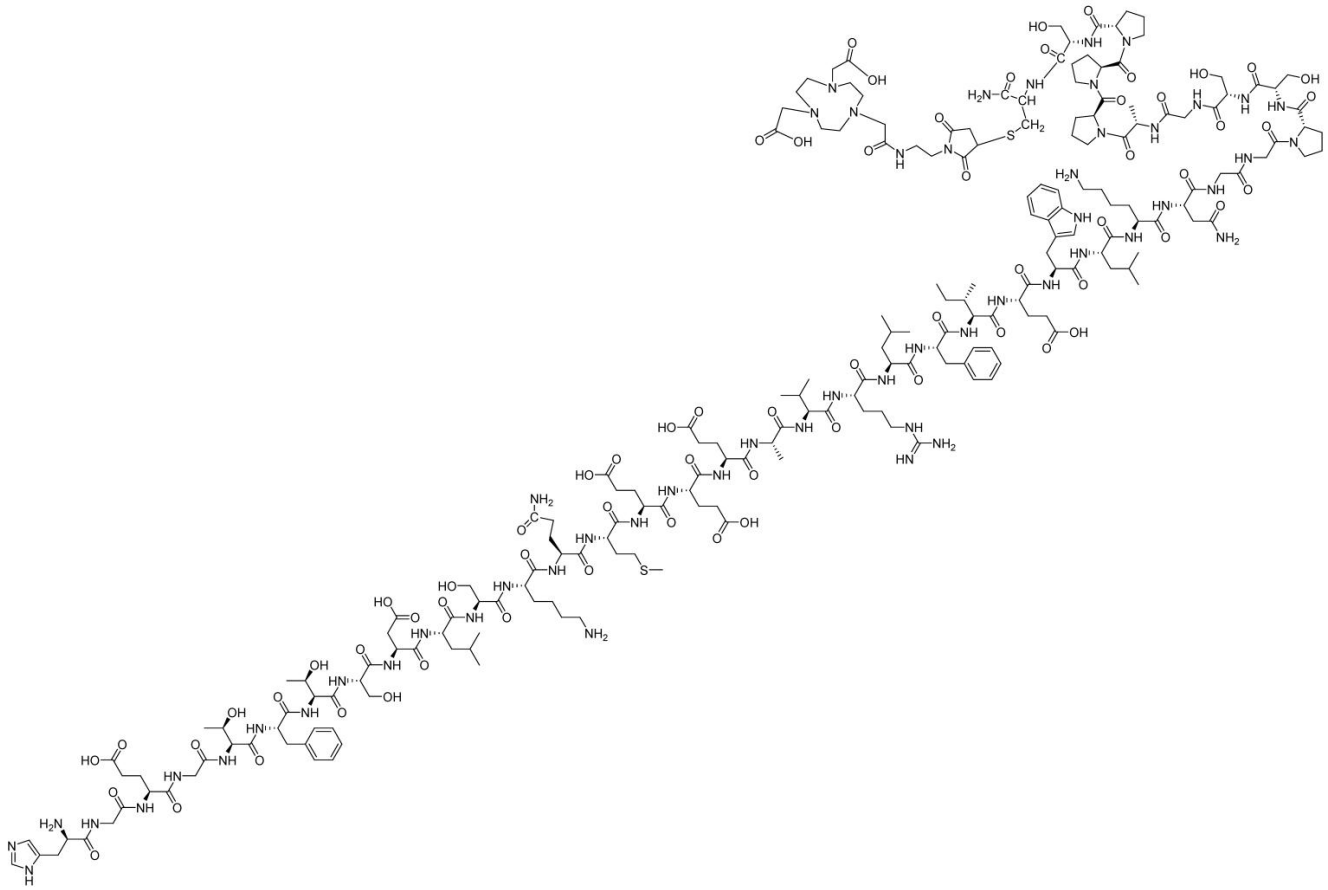

Figure 1. Structure of NOTA-MAL-cys^{40}-exendin-4 peptide.

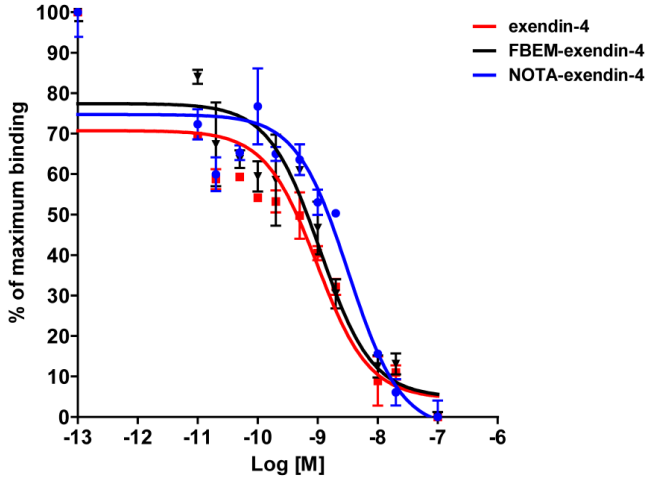

Figure 2. Affinity to INS-1 cells expressing GLP-1 receptor. Competitive binding study used [^{125}I]GLP-1 to provide comparison to the various exendin-4 analogs.

Preliminary biological analyses.

Cell binding studies were performed to confirm the retention of binding affinity (figure 2). Affinities were determined by competition with [^{125}I]GLP-1. The affinities (IC_{50}) for exendin-4, FBEM-cys^{40}-exendin-4, and NOTA-cys^{40}-exendin-4 were 0.98, 1.10, and 2.84 nM, respectively. [^{18}F]AlF-NOTA-MAL-cys^{40}-exendin-4 proved to be stable in human plasma at 37°C for up to one hour (data not shown).

PET Imaging of Insulinoma INS-1 Xenograft Model.

Representative coronal PET/CT image at 60 min and PET images at both 30 min and 60 min are shown in figure 3A. The receptor specificity of the tracer accumulation was confirmed by a blocking study, in which 100 µg exendin-4 was pre-injected. The PET images showed high tumor uptake into INS-1 insulinoma xenografts of 15.7 ± 1.4 % ID/g at 30 min and 14.6 ± 1.3 % ID/g at 60 min (figure 3B). Following a blocking dose, the tumor uptake of [^{18}F]AlF-NOTA-MAL-cys^{40}-exendin-4 was significantly lower ($p < 0.01$) than that of unblocked tumors at both time points tested (0.51 ± 0.05 %ID/g at 30 min and 0.20 ± 0.02 %ID/g at 60 min p.i.). Radioactivity accumulation in the kidneys was extremely high. The results of the ex vivo biodistribution study of Al[^{18}F]F-NOTA-MAL-cys^{40}-exendin-4 are shown in figure 3C. These results were consistent with PET imaging data and tumor uptake was 17.9 ± 1.4 %ID/g. In blocking study, the tumor uptake was decreased to 0.18 ± 0.02 %ID/g. Uptake was also significantly inhibited in the lung, pancreas, and stomach. No uptake inhibition occurred in the kidneys.

Dynamic PET scanning showed the relative rates of uptake in various tissues (figure 4A). Tumor uptake reached a plateau by about 5 min. All other major tissues, except for the kidneys, peaked early and then cleared over one hour. The blood clearance of the tracer was very fast and the majority of activity was taken up by kidneys. Uptake in the kidneys continued to increase throughout the course of the experiment. Quantification of PET images at the 1 h time point showed favorable tumor-to-muscle (175.8 ± 26.4) and tumor-to-liver (31.5 ± 6.7) radioactivity ratios. Biodistribution study by tissue dissection provided similar tumor-to-muscle and tumor-to-liver radioactivity ratios of 286.2 ± 33.3 and 45.8 ± 7.2, respectively (figure 4B).

Metabolites.

Extracts of plasma, tumor, kidneys, and urine, harvested at 1 h post-injection were analyzed for radiochemical components by radio-HPLC (figure 5). Extraction efficiencies were 78.3%, 71.9%, and 60.4% from plasma, tumor, and kidneys, respectively. Plasma and tumor contained a significant proportion of parent peptide, 74% and 64%, respectively; the remainder being a single polar radioactive metabolite peak. These percentages may be an overestimation of parent content if the extraction efficiency of the polar component was lower than the parent. Kidney extracts and urine extracts contained only polar metabolite. Kidney uptake, determined by analysis of PET images, following injection of [^{18}F]AlF-NOTA-MAL-cys^{40}-exendin-4, showed values of 79.25 ± 3.67 %ID/g and 74.68 ± 6.20 %ID/g at 30 min and 60 min, respectively. Co-injection of polyglutamic acid solution, in an effort to reduce kidney uptake [14], resulted in 25% inhibition. The uptake values, following blocking, were 58.44 ± 4.07 %ID/g ($p = 0.00086$) and 58.03 ± 2.59 %ID/g ($p = 0.0078$) at 30 min and 60 min p.i., respectively (figure 6).

Kidney extracts were analyzed by LC-MS and compared with extracts from control kidney harvested from an animal that had not been injected with the radiotracer. Unfortunately, extracts from the control kidney gave variable background results. Thus, we were unable to define or identify any metabolic component that co-eluted with the radioactivity. However, it did lead us to examine the kidney uptake of [^{18}F]AlF-NOTA-MAL-cys^{0}-exendin-4 in non-tumor bearing mice. This isomer has the NOTA attached at the N-terminus of the peptide. [^{18}F]AlF-NOTA-cys^{0}-exendin-4 also showed high and sustained kidney uptake of 58.5 ± 5.86 and 62.5 ± 13.1 %ID/g at 30 and 60 min p.i., respectively.

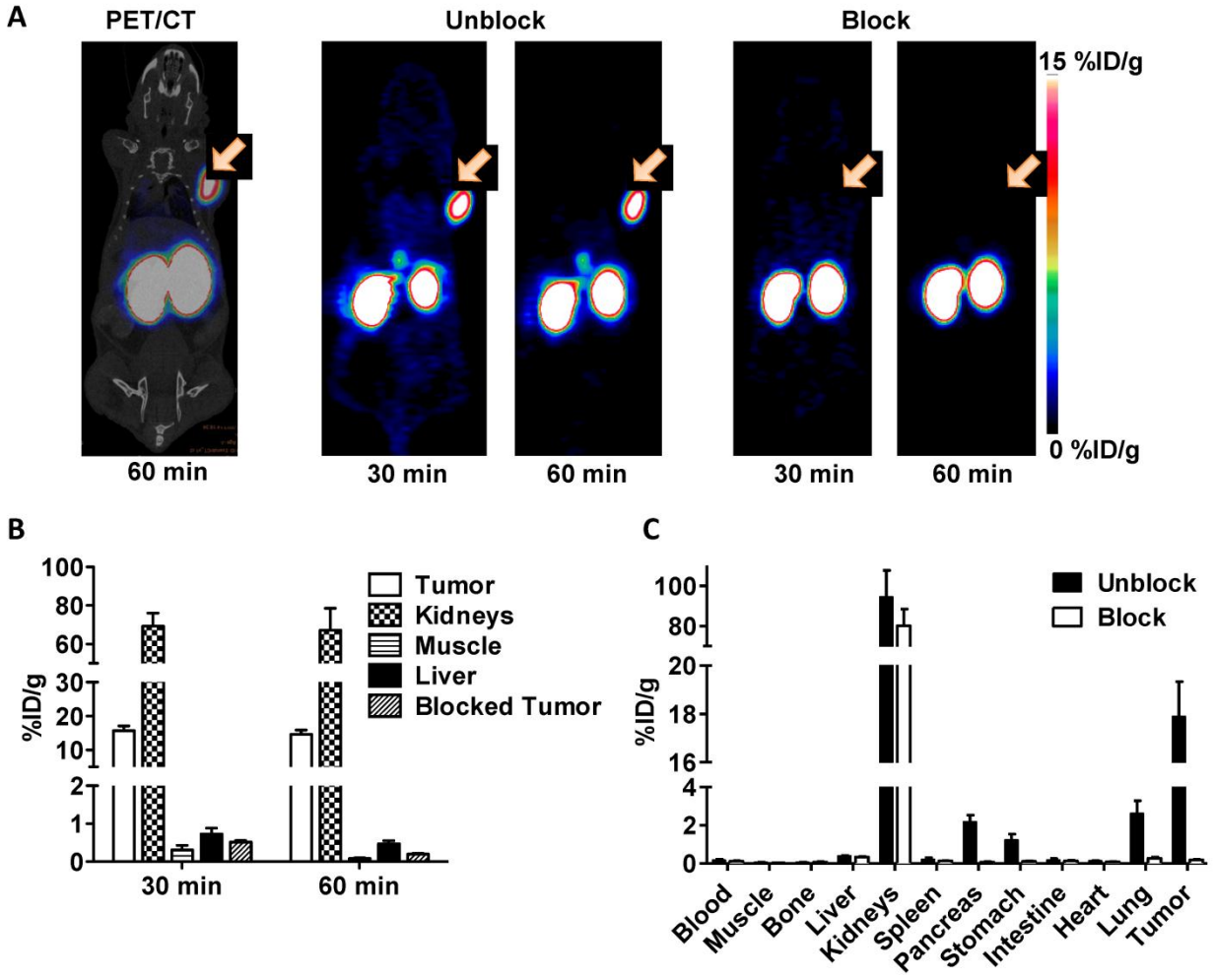

Figure 3. A) Representative PET images of [^{18}F]AlF-NOTA-MAL-cys^{40}-exendin-4 in INS-1 xenografted mice at 30 and 60 min p.i.. Tumor uptake is completely blocked by co-administration of a blocking dose of exendin-4. B) Quantification of uptake by selected tissues determined by ROIs following injection of [^{18}F]AlF-NOTA-MAL-cys^{40}-exendin-4 or co-injection of blocking agent (exendin-4) into INS-1 tumor-bearing mice at 30 and 60 min p.i.. C) Experiment of B at 60 min with analysis by tissue dissection and gamma counting.

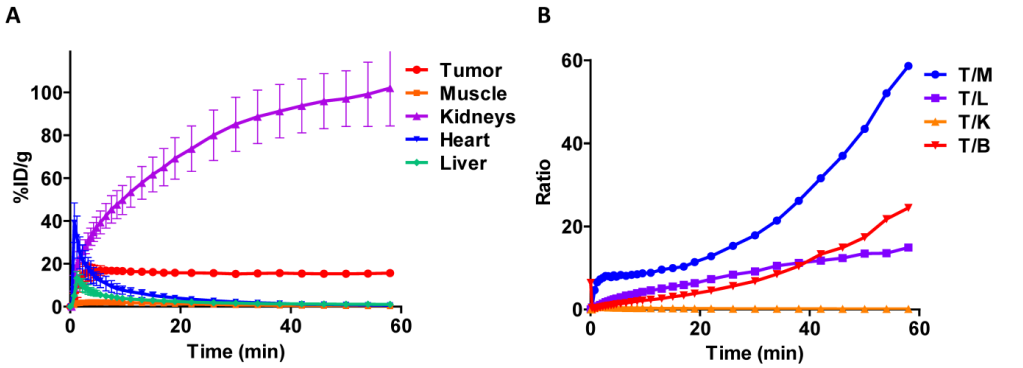

Figure 4. A) Tissue time-activity curves generated from dynamic imaging studies following injection of [^{18}F]AlF-NOTA-MAL-cys^{40}-exendin-4. B) Tumor-to-tissue activity ratios at 60 min p.i. T/M - tumor to muscle; T/L - tumor to liver; T/K - tumor to kidney; T/B - tumor to blood.

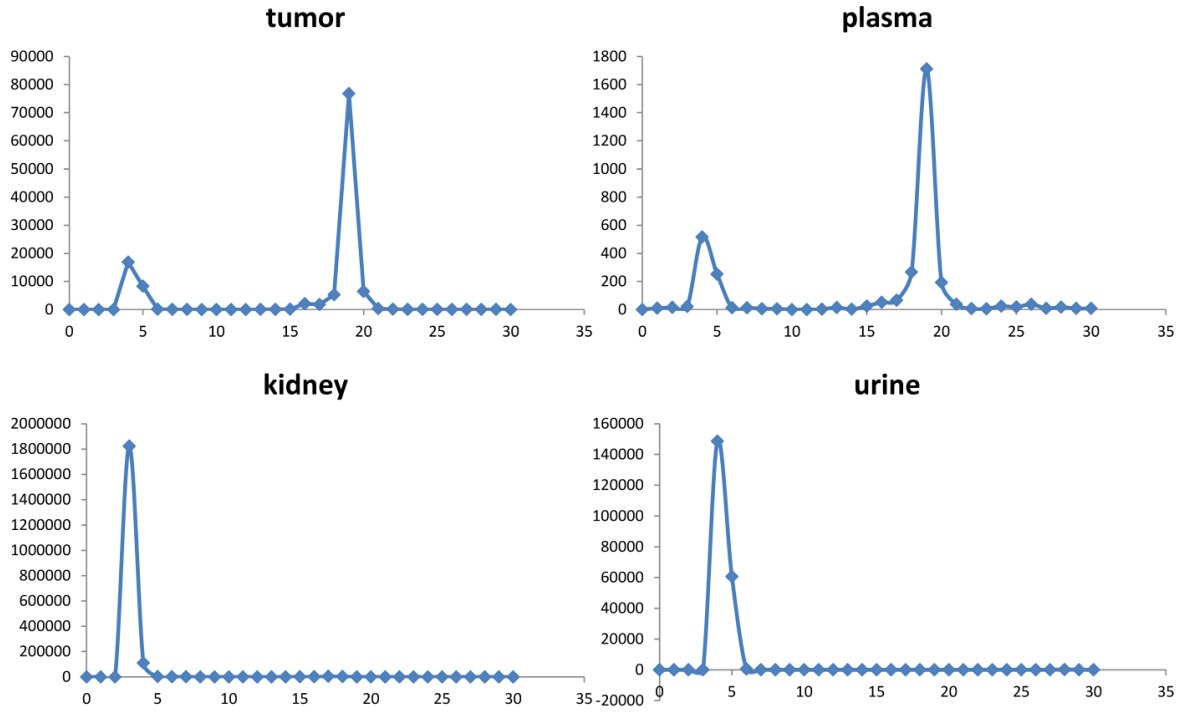

Figure 5. Radiochromatograms of tissue extracts harvested at 60 min.

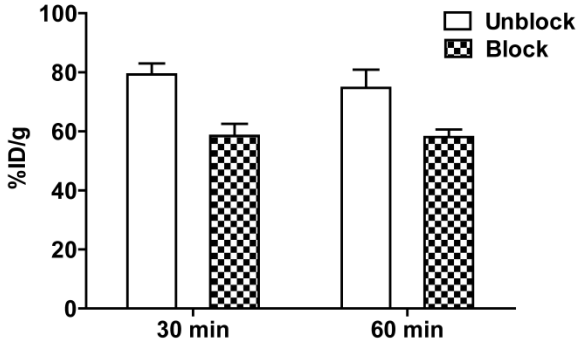

Figure 6. Reduction of kidney uptake observed 30 and 60 min p.i. upon co-injection of 8 mg polyglutamic acid with [^{18}F]AlF-NOTA-MAL-cys^{40}-exendin-4.

Discussion

Metal chelation chemistry has been utilized extensively for radiolabeling purposes, both for diagnostic and therapeutic applications. ^{99m}Tc and ^{111}In are widely used in single photon emission computed tomography (SPECT) realm [18]. The use of rapid chelation for PET radiochemicals has become more common with the availability of ^{64}Cu [19], ^{68}Ga [20], ^{89}Zr [21], and the recently introduced aluminum [^{18}F]fluoride complex with NOTA [17, 22].

GLP-1 analogs have been radiolabeled with ^{111}In [12-14] and ^{68}Ga [14, 23]. These compounds are effective for imaging insulinoma and may have utility for pancreatic beta-cell imaging, but do suffer from high kidney uptake. The ^{111}In labeled derivatives may also be applied therapeutically with the caveat that high kidney doses may cause unwanted side effects [13]. In a previous study, we developed two classes of GLP-1R binding peptides and incorporated a single cysteine residue, which allowed application of our cysteine specific, fluorine-18 radiolabeled maleimide [15, 24]. The best of the three analogs we prepared, [^{18}F]FBEM-cys^{40}-exendin-4, showed excellent uptake into INS-1 tumor xenografts [15]. Uptake in the kidneys was also high, but significant clearance from the kidneys was observed over the 2-h imaging studies. The clearance from the kidneys was much greater than clearance from the INS-1 xenograft.

[^{18}F]AlF-NOTA-MAL-cys^{40}-exendin-4 was found to exhibit biological properties similar to those of our previous exendin-4 analogs. The binding affinity to

INS-1 cells was about 2.5 times lower, but the IC_{50} was still a respectable 2.84 nM. Uptake into INS-1 xenografts following intravenous injection represented specific binding as the uptake could be blocked by co-injection of 100 μg of exendin-4. The tracer rapidly cleared from background tissues with the exception of the kidneys.

Human dosimetry calculations will be required to determine whether kidney uptake will adversely impact the potential utility of this radiotracer. However, the high kidney uptake, exhibited by this analog, was much lower than that reported in the literature for ^{68}Ga and ^{111}In analogs [25]. Kidney uptake of ^{111}In-DTPA-exendin-4 C-terminal analog was 208 %ID/g at 4 h p.i. and decreased to 104 %ID/g by 24 h [12]. Similarly, the ^{68}Ga-DOTA C-terminal analog of exendin-3 showed 120 %ID/g at 60 min p.i. [23]. These authors also showed that the ^{111}In-DOTA version had similar kidney uptake. The lowest kidney uptake reported to date was for our [^{18}F]FBEM-cys^{40}-exendin-4, which showed kidney uptake of 13.2 and 4.2 %ID/g at 60 and 120 min p.i., respectively [15].

In a previous report by Wild et al. [14], kidney uptake could be reduced by 49% by immediate pre-injection with polyglutamic acid. We were able to realize a 25% inhibition of kidney uptake upon co-injection of polyglutamic acid following the literature protocol. Based on the specific activity of our preparation, the mass dose of exendin-4 peptide was approximately 300 pmol or 20 times more mass than that used by Wild et al. [14].

In our studies, kidney extract showed a single very polar radioactive metabolite and no parent peptide was detected. We made an attempt to the identity of the trapped chemical entity by comparing HPLC-MS traces of kidney extract from an animal that had received [^{18}F]AlF-NOTA-MAL-cys^{40}-exendin-4 with that from an animal that had not been injected. We were not able to identify any metabolic species in these extracts.

Still operating on the hypothesis that the high kidney uptake was due to a highly retained metabolite, we prepared the isomeric [^{18}F]AlF-NOTA-MAL-cys^{0}-exendin-4. This isomer should not yield any identical radiolabeled peptide fragments. The kidney uptake for this isomer was still very high, but only 60 %ID/g at 1 hour. We cannot state whether this slightly lower uptake was due to less kidney uptake initially or to faster clearance into the urine.

Thus, the metabolic species contributing to high kidney uptake remains unidentified. Since we are able to extract parent compound from tumor and plasma, the kidney uptake is not caused by uptake of parent compound. The general observation that exendin-4 peptides containing a C-terminal chelated radiometal show very high uptake suggests that some metabolite from the C-terminal end is responsible for this very slow egress from the kidneys.

The driving force for the development of this NOTA-maleimide analog of cys^{40}-exendin-4 was the ease of radiochemical synthesis. The multidentate chelator NOTA allows radiolabeling with positron-emitting radionuclides ^{68}Ga, ^{64}Cu, and [^{18}F]AlF using rapid synthetic reactions [20, 26]. ^{68}Ga, a generator produced radionuclide, is becoming much more readily available. Chelation reactions with NOTA are generally fast and efficient. However, the 68-min half-life may limit some applications to human imaging.

^{64}Cu, with its 12.8 h half-life and low proportion of positron-emission (17.4 %), has generated much interest due to facile chelation chemistry and utility for imaging kinetically slower processes. Copper radiolabeled compounds tend to exhibit high liver uptake presumably as a result of transchelation of the copper radionuclide [19], [27]. Intensive studies to prepare new chelators with higher kinetic stability have resulted in improvements, but the problem is not completely solved [19], [28]. The transchelation, coupled with the large number of radioactive decay emissions, compromises signal to background and may result in unacceptable radiation dose to patients.

[^{18}F]Fluoride is readily available from cyclotron production and can be obtained from commercial cyclotron facilities. This radionuclide has appropriate positron emission energy (633 keV) and positron abundance (97%). Complexation with [^{18}F]AlF is a simple procedure. For typical syntheses, aqueous fluoride was added to the precursor at pH 4 and the mixture heated for 10 min. Purifications were typically conducted with solid-phase-extraction (SPE). However, NOTA-MAL-cys^{40}-exendin-4 is not a typical peptide. The radiolabeling conditions resulted in a number of radiolabeled side products, which required HPLC purification in order to achieve high radiochemical purity. In our previous studies with [^{18}F]FBEM-exendin-4, presumed oxidation of the methionine caused degradation of the final product during concentration [15]. In the course of this work, we determined that stability of the product was enhanced by conducting the final concentration step in the presence of a pH 4 buffer; very little sulfur oxidation impurity was observed.

The radiochemical yield was sensitive to the quantity of target water and to the amount of substrate used. We did not attempt to increase the concentration of [^{18}F]fluoride using trap and release

methods. Because we cannot chromatographically separate unconsumed starting material or fluorinated from non-fluorinated complex, the quantity of substrate used dictated the ultimate specific activity.

Our procedure for preparation of FBEM-cys^{40}-exendin-4 required the synthesis of [^{18}F]FBEM via an automated synthesis device followed by the coupling reaction and HPLC purification. [^{18}F]FBEM was prepared in less than 20% yield (uncorrected) in approximately 100 min. Coupling to peptide and purification was achieved in less than 35% yield (uncorrected) and consumed almost another 60 min prior to delivery for animal studies. Thus, the overall uncorrected yield from [^{18}F]fluoride was about 5% and required over 2.5 h. On the contrary, the [^{18}F]AlF complexation reaction described in this manuscript required about 35 min from start of synthesis to isolated HPLC fraction. An additional 20 min was required for isolation and concentration for small animal studies. The uncorrected radiochemical yield was approximately 23%. This procedure had a significant reduction in time required for the synthesis and an improved uncorrected radiochemical yield.

Conclusions

[^{18}F]AlF-NOTA-MAL-Cys^{40}-exendin-4 displayed similar biological properties compared to [^{18}F]FBEM-cys^{40}-exendin-4, with the exception of much higher kidney uptake. Receptor affinity for GLP-1R and uptake into INS-1 xenograft tumors were very similar. The attractiveness of this radioligand for further evaluation stems from its biological properties and its relative ease of radiochemical synthesis compared to other fluorine-18 ligands for GLP-1R.

Acknowledgements

This research was supported by the intramural research program of the National Institute of Biomedical Imaging and Bioengineering, NIH. Fluorine-18 was prepared by the cyclotron facility of the Positron Emission Tomography Department, Warren Grant Magnuson Clinical Center, NIH.

Competing Interests

The authors have declared that no competing interest exists.

References

1. Fowler JS, Wolf AP. Working against time: Rapid radiotracer synthesis and imaging the human brain. Acc Chem Res. 1997; 30: 181-8.
2. Holst JJ, Deacon CF, Vilsboll T, Krarup T, Madsbad S. Glucagon-like peptide-1, glucose homeostasis and diabetes. Trends in Molecular Medicine. 2008; 14: 161-8.
3. Tornehave D, Kristensen P, Romer J, Knudsen LB, Heller RS. Expression of the GLP-1 Receptor in Mouse, Rat, and Human Pancreas. J Histochem Cytochem. 2008; 56: 841-51..
4. Reubi JC, Waser B. Concomitant expression of several peptide receptors in neuroendocrine tumours: molecular basis for in vivo multireceptor tumour targeting. Eur J Nucl Med Mol Imaging. 2003; 30: 781-93.
5. Ban K, Noyan-Ashraf MH, Hoefer J, Bolz SS, Drucker DJ, Husain M. Cardioprotective and vasodilatory actions of glucagon-like peptide 1 receptor are mediated through both glucagon-like peptide 1 receptor-dependent and -independent pathways. Circulation. 2008; 117: 2340-50.
6. Chatziioannou A, Kehagias D, Mourikis D, Antoniou A, Limouris G, Kaponis A, et al. Imaging and localization of pancreatic insulinomas. Clin Imaging. 2001; 25: 275-83.
7. Deacon CF, Johnsen AH, Holst JJ. Degradation of glucagon-like peptide-1 by human plasma in-vitro yields an N-terminally truncated peptide that is a major endogenous metabolite in-vivo. J Clin Endocrinol Metab. 1995; 80: 952-7.
8. Murage EN, Gao G, Bisello A, Ahn JM. Development of potent glucagon-like peptide-1 agonists with high enzyme stability via introduction of multiple lactam bridges. J Med Chem. 2010; 53: 6412-20.
9. Kiesewetter DO, Jacobson O, Lang L, Chen X. Automated radiochemical synthesis of [^{18}F]FBEM: A thiol reactive synthon for radiofluorination of peptides and proteins. Appl Radiat Isot. 2011; 69: 410-4.
10. Gao H, Niu G, Yang M, Quan Q, Ma Y, Murage EN, et al. PET of insulinoma using [^{18}F]-FBEM-EM3106B, a new GLP-1 analogue. Mol Pharm. 2011; 8: 1775-82.
11. Nielsen LL, Young AA, Parkes DG. Pharmacology of exenatide (synthetic exendin-4): a potential therapeutic for improved glycemic control of type 2 diabetes. Regul Pept. 2004; 117: 77-88.
12. Wild D, Behe M, Wicki A, Storch D, Waser B, Gotthardt M, et al. [Lys^{40}(Ahx-DTPA-^{111}In)NH$_2$]exendin-4, a very promising ligand for glucagon-like peptide-1 (GLP-1) receptor targeting. J Nucl Med. 2006; 47: 2025-33.
13. Wicki A, Wild D, Storch D, Seemayer C, Gotthardt M, Behe M, et al. [Lys^{40}(Ahx-DTPA-111In)NH2]-Exendin-4 is a highly efficient radiotherapeutic for glucagon-like peptide-1 receptor-targeted therapy for insulinoma. Clin Cancer Res. 2007; 13: 3696-705.
14. Wild D, Wicki A, Mansi R, Behe M, Keil B, Bernhardt P, et al. Exendin-4-based radiopharmaceuticals for glucagonlike peptide-1 receptor PET/CT and SPECT/CT. J Nucl Med. 2010; 51: 1059-67.
15. Kiesewetter DO, Gao H, Ma Y, Niu G, Quan Q, Guo N, et al. ^{18}F-radiolabeled analogs of exendin-4 for PET imaging of GLP-1 in insulinoma. Eur J Nucl Med Mol Imaging. 2012; 39: 463-73.
16. Gao H, Kiesewetter DO, Zhang X, Huang X, Guo N, Lang L, et al. PET imaging of glucagon-like peptide receptor upregulation after myocardial ischemia/reperfusion injury. J Nucl Med. 2012; in press.
17. McBride WJ, Sharkey RM, Karacay H, D'Souza CA, Rossi EA, Laverman P, et al. A novel method of ^{18}F radiolabeling for PET. J Nucl Med. 2009; 50: 991-8.
18. Fani M, Maecke HR. Radiopharmaceutical development of radiolabelled peptides. Eur J Nucl Med Mol Imaging. 2012; 39: 11-30.
19. Shokeen M, Anderson CJ. Molecular imaging of cancer with copper-64 radiopharmaceuticals and positron emission tomography (PET). Acc Chem Res. 2009; 42: 832-41.
20. Breeman WAP, de Blois E, Chan HS, Konijnenberg M, Kwekkeboom DJ, Krenning EP. Ga-68-labeled DOTA-Peptides and Ga-68-labeled radiopharmaceuticals for positron emission tomography: Current status of research, clinical applications, and future perspectives. Semin Nucl Med. 2011; 41: 314-21.
21. Holland JP, Sheh Y, Lewis JS. Standardized methods for the production of high specific-activity zirconium-89. Nucl Med Biol. 2009; 36: 729-39.
22. McBride WJ, D'Souza CA, Sharkey RM, Karacay H, Rossi EA, Chang CH, et al. Improved ^{18}F labeling of peptides with a fluoride-aluminum-chelate complex. Bioconjug Chem. 2010; 21: 1331-40.
23. Brom M, Oyen WJ, Joosten L, Gotthardt M, Boerman OC. ^{68}Ga-labelled exendin-3, a new agent for the detection of insulinomas with PET. Eur J Nucl Med Mol Imaging. 2010; 37: 1345-55.
24. Gao H, Niu G, Yang M, Quan Q, Ma Y, Murage EN, et al. PET of insulinoma using ^{18}F-FBEM-EM3106B, a new GLP-1 analogue. Mol Pharm. 2011; 8: 1775-82.
25. Vegt E, van Eerd JE, Eek A, Oyen WJ, Wetzels JF, de Jong M, et al. Reducing renal uptake of radiolabeled peptides using albumin fragments. J Nucl Med. 2008; 49: 1506-11.
26. Fani M, Andre JP, Maecke HR. ^{68}Ga-PET: a powerful generator-based alternative to cyclotron-based PET radiopharmaceuticals. Contrast Media Mol Imaging. 2008; 3: 67-77.

27. Liu Z, Yan Y, Liu S, Wang F, Chen X. F-18, Cu-64, and Ga-68 Labeled RGD-Bombesin Heterodimeric Peptides for PET Imaging of Breast Cancer. Bioconjug Chem. 2009; 20: 1016-25.
28. Garrison JC, Rold TL, Sieckman GL, Figueroa SD, Volkert WA, Jurisson SS, et al. In vivo evaluation and small-animal PET/CT of a prostate cancer mouse model using Cu-64 bombesin analogs: Side-by-side comparison of the CB-TE2A and DOTA chelation systems. J Nucl Med. 2007; 48: 1327-37.